Revision 1

Ebnerite and epiebnerite: NH_4ZnPO_4 dimorphs with zeolite-type frameworks from the Rowley mine, Arizona, USA

Anthony R. Kampf[1*], Xiangping Gu[2], Hexiong Yang[3], Chi Ma[4] and Joe Marty[1]

[1] Mineral Sciences Department, Natural History Museum of Los Angeles County, 900 Exposition Boulevard, Los Angeles, California 90007, USA

[2] School of Geosciences and Info-Physics, Central South University, Changsha, Hunan 410083, China

[3] Department of Geosciences, University of Arizona, 1040 E. 4th Street, Tucson, AZ 85721-0077, USA

[4] Division of Geological and Planetary Sciences, California Institute of Technology, 1200 East California Boulevard, Pasadena, California 91125, USA

*E-mail: akampf@nhm.org

Abstract

Ebnerite and epiebnerite, both with the ideal formula NH_4ZnPO_4, are new mineral species from the Rowley mine, Maricopa County, Arizona, U.S.A. They occur in an unusual bat-guano-related, post-mining assemblage of phases. Epiebnerite grows epitactically on

This is a 'preproof' accepted article for Mineralogical Magazine. This version may be subject to change during the production process.
DOI: 10.1180/mgm.2024.15

ebnerite and replaces it. Ebnerite and epiebnerite are found in intimate association with alunite, halite, mimetite, newberyite, sampleite, struvite and wulfenite on hematite-rich quartz-barite matrix. Crystals of ebnerite are colourless narrow prisms up to about 0.3 mm in length. The streak is white, luster is vitreous, Mohs hardness is ~2, tenacity is brittle and fracture is splintery. The density is 2.78(2) g·cm^{-3}. Ebnerite is optically uniaxial (–) with ω = 1.585(2) and ε = 1.575(2). Epiebnerite occurs as colourless prisms or blades, up to about 10 x 3 x 2 μm, in parallel growth forming ribs with serrated edges epitactic on ebnerite prisms. The streak is white, luster is vitreous, Mohs hardness is probably ~2, tenacity is brittle. The calculated density is 2.851 g·cm^{-3}. Epiebnerite is optically biaxial with all indices of refraction near 1.580. Electron microprobe analysis gave the empirical formula $[(NH_4)_{0.89}K_{0.06}]_{\Sigma 0.95}(Zn_{0.96}Cu_{0.07})_{\Sigma 1.03}[(P_{0.97}Si_{0.03})_{\Sigma 1.00}O_4]$ for ebnerite and $[(NH_4)_{0.67}K_{0.28}]_{\Sigma 0.95}(Zn_{0.99}Cu_{0.02})_{\Sigma 1.02}(P_{1.00}O_4)$ for epiebnerite. Ebnerite is hexagonal, $P6_3$, with a = 10.67051(16), c = 8.7140(2) Å, V = 859.25(3) Å^3 and Z = 8. Epiebnerite is monoclinic, $P2_1$, with a = 8.796(16), b = 5.457(16), c = 8.960(16) Å, β = 90.34(6)°, V = 430.1(17) Å^3 and Z = 4. The structures of ebnerite (R_1 = 0.0372 for 1168 $I_o > 2\sigma I$ reflections) and epiebnerite (known from synthetic monoclinic NH_4ZnPO_4) are zeolite-like frameworks based upon corner-sharing linkages between alternating ZnO_4 and PO_4 tetrahedra with channels in the frameworks hosting the NH_4 groups. The two structures are topologically distinct. Ebnerite belongs to the family of "stuffed derivatives" of tridymite, whereas epiebnerite possesses an ABW-type zeolite.

Keywords: ebnerite; epiebnerite; zeolite-like framework; tridymite stuffed derivative; ABW-type zeolite; NH_4ZnPO_4–HEX; NH_4ZnPO_4–ABW; new mineral species; phosphate; crystal structure; Rowley mine, Arizona.

https://doi.org/10.1180/mgm.2024.15 Published online by Cambridge University Press

Introduction

The NH_4ZnPO_4 dimorphs ebnerite and epiebnerite are new mineral species with zeolite-like framework structures found in an unusual bat guano assemblage in the Rowley mine in southwestern Arizona (USA). The ebnerite structure belongs to the family of "stuffed derivatives" of tridymite (Buerger, 1954). Epiebnerite has an ABW-type zeolite structure (Bu *et al*., 1997; Kahlenberg *et al*., 2001).

The name ebnerite honours John Ebner of Tucson, Arizona, USA (b. 1931). Mr. Ebner has been an avid mineral collector for more than 65 years and has focused on micro-minerals for the last 41 years. He has developed one of the most significant micromount collections in the world, now numbering well over 50,000, and has also dedicated himself to documenting and preserving the knowledge and history of micromounting. In 1997, he was inducted into the Micromounts Hall of Fame. Mr. Ebner has contributed immensely to the amateur mineral community, writing articles, presenting programs, organizing symposia, serving as an officer in many clubs, etc. He has also contributed significantly to mineralogical science in a variety of ways, such as providing specimens for study and volunteering his services. Mr. Ebner has been a volunteer in the Department of Geosciences and the mineral museum at the University of Arizona since 2016. Mr. Ebner has agreed to the naming of the mineral in his honour. The name epiebnerite is a combination of the prefix 'epi' for 'near' in Greek and the mineral name "ebnerite" because the mineral is the dimorph of ebnerite. 'Epi' also alludes to the fact that the mineral has only been found growing epitaxially on ebnerite or forming epimorphs after ebnerite.

The new minerals and their names were approved by the Commission on New Minerals, Nomenclature and Classification of the International Mineralogical Association (IMA 2022-123 and IMA 2023-066, respectively). Two cotype specimens of ebnerite are deposited in the collections of the Natural History Museum of Los Angeles County, Los

https://doi.org/10.1180/mgm.2024.15 Published online by Cambridge University Press

Angeles, California, USA, catalogue numbers 76275 and 76276. One cotype specimen of ebnerite is deposited at the University of Arizona Alfie Norville Gem and Mineral Museum, catalogue number 22729 and one cotype specimen is deposited at the RRUFF Project (https://rruff.info/), deposition number R220032. Four cotype specimens of epiebnerite are deposited in the collections of the Natural History Museum of Los Angeles County, Los Angeles, California, USA, catalogue numbers 76294, 76295, 76296 and 76297.

Occurrence

Ebnerite and epiebnerite were collected by one of the authors (JM) on the 125-foot level of the Rowley mine, about 20 km NW of Theba (small settlement and railroad depot), Maricopa County, Arizona, USA (33°2'57"N 113°1'49.59"W). The Rowley mine is on the western slope of the Painted Rock Mountains (in the Painted Rock mining district) and overlooks the Dendora Valley, immediately to the west. It is a former Cu-Pb-Au-Ag-Mo-V-baryte-fluorspar mine that exploited veins presumed to be related to the intrusion of an andesite porphyry dike into Tertiary volcanic rocks. Although the mine has not been operated for ore since 1923, collectors took notice of the mine as a source of fine wulfenite crystals around 1945. An up-to-date account of the history, geology and mineralogy of the mine was recently published by Wilson (2020).

The new minerals were found in a hot and humid area of the mine (see Fig. 26 in Wilson, 2020) in an unusual bat guano-related, post-mining assemblage of phases that include a variety of vanadates, phosphates, oxalates and chlorides, some containing $(NH_4)^+$. This secondary mineral assemblage is found growing on baryte-quartz-rich matrix and, besides ebnerite and epiebnerite, includes allantoin (Kampf *et al*., 2021a), alunite, ammineite, antipinite, aphthitalite, bassanite, biphosphammite, carboferriphoxite (Kampf *et al*., 2024a), cerussite, davidbrownite-(NH_4) (Kampf *et al*., 2019a), dendoraite-(NH_4) (Kampf *et al*.,

https://doi.org/10.1180/mgm.2024.15 Published online by Cambridge University Press

2022a), edwindavisite (Yang *et al*., 2023a), ferriphoxite (Kampf *et al*., 2024b), fluorite, halite, hydroglauberite, mimetite, mottramite, natrosulfatourea (Kampf *et al*., 2021a), newberyite, perite, phoxite (Kampf *et al*., 2019b), relianceite-(K) (Kampf *et al*., 2022b), rowleyite (Kampf *et al*., 2017), salammoniac, sampleite, struvite, thebaite-(NH_4) (Kampf *et al*., 2021b), thenardite, urea, vanadinite, weddellite, willemite, wulfenite and several other potentially new minerals. Ebnerite and epiebnerite are both rare and have been found on only a handful of specimens. Ebnerite has been found without epiebnerite; however, epiebnerite has only been found growing on and/or replacing ebnerite. Because of the apparently consistent orientation of epiebnerite crystals on ebnerite, we interpret them to be epitactic overgrowths and/or epimorphs. Both minerals are found in intimate association with alunite, halite, mimetite, newberyite, sampleite, struvite and wulfenite on hematite-rich quartz-barite matrix. It is worth noting that groups of ebnerite crystals without epiebnerite overgrowths have been found immediately adjacent to ebnerite with epiebnerite overgrowths.

Physical and Optical Properties

Ebnerite

Crystals of ebnerite are colourless narrow prisms (often tapering), up to about 0.3 mm in length, typically forming fan- and bowtie-like sprays (Fig. 1). Although terminations appear irregular under moderate magnification, under high magnification, they are observed to consist of a hexagonal pyramid and/or a basal pedion. The Bravais–Friedel–Donnay–Harker principle (Donnay and Harker, 1937) predicts the {100} hexagonal prism and {101} hexagonal pyramid as the prominent forms, which is consistent with SEM observations of ebnerite crystals. The {001} basal pedion is also clearly present based on SEM observations (Figs. 2 and 3). The non-centrosymmetric space group suggests hemimorphic morphology; however, doubly terminated crystals have not been observed and the Bravais–Friedel–

https://doi.org/10.1180/mgm.2024.15 Published online by Cambridge University Press

Donnay–Harker principle indicates positive and negative forms to be equally probable. Therefore, to the above forms can be added {10-1} and {00-1}.

Ebnerite has a white streak, vitreous luster, brittle tenacity and splintery fracture. The Mohs hardness is about 2 based on scratch tests. Although no cleavage direction could be determined, the splintery fracture suggests at least one good cleavage in the [001] zone – possibly {100}. The mineral does not fluoresce in either long- or short-wave ultraviolet illumination. The density measured by flotation in a mixture of methylene-iodide and toluene is 2.78(2) $g \cdot cm^{-3}$. At room-temperature, ebnerite is insoluble in H_2O, but easily soluble in dilute HCl.

Ebnerite is optically uniaxial (–) with $\omega = 1.585(2)$ and $\varepsilon = 1.575(2)$ and it is nonpleochroic. The Gladstone-Dale comaptibility (Mandarino, 2007), $1 - (K_p/K_c)$, is 0.010 in the range of superior compatibility for the empirical formula.

Epiebnerite

Epiebnerite occurs as colourless prisms or blades, up to about 10 x 3 x 2 μm, in parallel growth forming ribs with serrated edges epitactic on ebnerite prisms or forming epimorphs after ebnerite (Fig. 4). No forms could be measured because of the minute size of crystals. The Bravais–Friedel–Donnay–Harker principle (Donnay and Harker, 1937) predicts that prisms are likely to be elongated on [010] with the prism the forms {100} and {001} and terminations consisting of the forms {110} and {011}. Synthetic crystals are reported to exhibit both racemic and rotational twinning (Bu *et al*., 1997). Note that we have been unable to define crystallographically the apparent epitactic relation between epiebnerite and ebnerite.

The streak is white, the luster is vitreous and the tenacity is brittle. The Mohs hardness is probably about 2, but crystals are too small to test. The density could not be measured because crystals are too small to see in density liquids. The calculated density is

https://doi.org/10.1180/mgm.2024.15 Published online by Cambridge University Press

2.851 g·cm^{-3}. At room-temperature, epiebnerite is insoluble in H_2O, but easily soluble in dilute HCl.

Complete optical determinations were impossible because of the minute size of the crystals; however, the average index of refraction is very close to 1.580 because crystals are virtually invisible in all orientations in the 1.580 immersion liquid. The Gladstone-Dale comaptibility (Mandarino, 2007), $1 - (K_p/K_c)$, is 0.012 in the range of superior compatibility for the empirical formula using $n_{av} = 1.580$.

Raman spectroscopy

Raman spectroscopy was conducted on a Horiba XploRA PLUS spectrometer using a 532 nm diode laser, 1800 gr/mm diffraction grating and a 100× (0.9 NA) objective. A 100 μm slit was used for ebnerite and a 200 μm slit was used for epiebnerite. Because crystals of epiebnerite are very sensitive to the laser, the spectrum was recorded at 2 mW power. Consequently, the epiebnerite spectrum exhibits significant noise, which makes it difficult to assign precise wavenumbers to the weaker bands. The spectra from 3700 to 60 cm^{-1} are shown in Figure 5 including labelled mode assignments based on several references: Frost *et al*. (2011), Sergeeva *et al*. (2019), Števko *et al*. (2018) and Yakovenchuk *et al*. (2018).

Chemical Analysis

Ebnerite analyses (4 points) were done on a Shimadzu EPMA-1720 electron microprobe in WDS mode. Analytical conditions were 15 kV accelerating voltage, 10 nA beam current and 2 μm beam diameter. Analytical data for ebnerite are given in Table 1. Epiebnerite analyses (4 points) were performed on a JEOL JXA-iHP200F electron microprobe in WDS mode. Analytical conditions were 15 kV accelerating voltage, 10 nA beam current and 10 μm beam diameter. It was impossible to polish epiebnerite crystals, so

https://doi.org/10.1180/mgm.2024.15 Published online by Cambridge University Press

analyses were done on unpolished crystal faces. Because of the uneven surfaces of epiebnerite crystals and their thinness, analytical values were significantly low, requiring normalization. The results are given in Table 2.

The empirical formulas for ebnerite and epiebnerite (based on O = 4 *apfu*) are $[(NH_4)_{0.89}K_{0.06}]_{\Sigma 0.95}(Zn_{0.96}Cu_{0.07})_{\Sigma 1.03}[(P_{0.97}Si_{0.03})_{\Sigma 1.00}O_4]$ and $[(NH_4)_{0.67}K_{0.28}]_{\Sigma 0.95}(Zn_{0.99}Cu_{0.02})_{\Sigma 1.02}(P_{1.00}O_4)$, respectively. The ideal formula for both is NH_4ZnPO_4, which requires $(NH_4)_2O$ 14.60, ZnO 45.62, P_2O_5 39.78, total 100 wt%.

X-ray crystallography

Powder X-ray studies were done using a Rigaku R-Axis Rapid II curved imaging plate microdiffractometer with monochromatized Mo*K*α radiation. A Gandolfi-like motion on the φ and ω axes was used to randomize the sample. The powder X-ray diffraction (PXRD) pattern for ebnerite closely matched that calculated from the crystal structure of synthetic hexagonal (HEX-type) NH_4ZnPO_4 (Harrison *et al*., 2001) and the PXRD pattern for epiebnerite closely matched that calculated from the crystal structure of synthetic monoclinic (ABW-type) NH_4ZnPO_4 (Bu *et al*., 1997). Observed *d*-values and intensities were derived by profile fitting using JADE Pro software (Materials Data, Inc.). The powder data for ebnerite and epiebnerite are presented in Supplementary Tables 1 and 2, respectively. Unit-cell parameters refined from the powder data using JADE Pro with whole pattern fitting are a = 10.6690(3), c = 8.727(3) Å, V = 863.7(5) Å^3 and Z = 8 for ebnerite (space group $P6_3$) and a = 8.796(16), b = 5.457(16), c = 8.960(16) Å, β = 90.34(6)°, V = 430.1(17) Å^3 and Z = 4 for epiebnerite (space group $P2_1$).

Single-crystal study of epiebnerite was not attempted because of the small size of crystals and their occurrence in subparallel intergrowths. Figure 6 shows the close match

https://doi.org/10.1180/mgm.2024.15 Published online by Cambridge University Press

between the epiebnerite PXRD and that calculated from the structure of synthetic monoclinic (ABW-type) NH_4ZnPO_4 (Bu *et al*., 1997) following the whole-pattern-fitting cell refinement.

Single-crystal X-ray studies for ebnerite were done using a Rigaku Xtalab Synerg D/S 4-circle diffractometer equipped with Cu*K*α radiation. The structure was solved using SHELXT (Sheldrick, 2015a). Refinement proceeded by full-matrix least-squares on F^2 using SHELXL-2016 (Sheldrick, 2015b). The two N sites were refined with joint occupancies by N and K. The occupancies of the two Zn and two P sites were refined, but joint occupancies were not employed because of the close correspondence in scattering power of Zn and Cu and of P and Si. The less-than-full refined occupancies obtained for the Zn and P sites are consistent with some substitution of Cu for Zn and Si for P, as indicated by the EPMA. All H atoms associated with the NH_4 groups were located through difference Fourier syntheses. The H sites were refined with soft restraints of 0.90(3) Å on the N–H distances and 1.45(3) Å on the H–H distances and with the U_{eq} of each H set to 1.2 times that of the associated N atom; the occupancies of the H sites were tied to those of the N sites. Data collection and refinement details are given in Table 3, atom coordinates and displacement parameters in Table 4, selected bond distances and angles in Table 5 and a bond valence analysis in Table 6. Note that, even though the location of H sites allowed the determination of the hydrogen bonding scheme thereby helping to understand how the NH_4 groups are bound in the channels, bond-valence calculations are more straightforward if the NH_4 groups are treated as spherical cations (see Garcia-Rodriguez *et al*., 2000).

Discussion of the structures

Both ebnerite and epiebnerite have zeolite-like framework structures based upon corner-sharing linkages between alternating ZnO_4 and PO_4 tetrahedra, with channels in the frameworks hosting the NH_4 groups. Their structures are similar to those of aluminosilicate

https://doi.org/10.1180/mgm.2024.15 Published online by Cambridge University Press

zeolites, although neither mineral is isostructural with any known mineral. As noted above, ebnerite is the natural counterpart of synthetic hexagonal NH_4ZnPO_4 (Harrison *et al*., 2001) and epiebnerite is the natural counterpart of synthetic monoclinic NH_4ZnPO_4 (Bu *et al*., 1997). Harrison *et al*. (2001) referred to hexagonal NH_4ZnPO_4 as NH_4ZnPO_4–HEX and monoclinic NH_4ZnPO_4 as NH_4ZnPO_4–ABW. The ABW suffix denotes the fact that the monoclinic phase has an ABW-type zeolite structure. The two structures are topologically distinct; the channels in the HEX (ebnerite) structure are defined by six-member rings of tetrahedra, whereas the channels in the ABW (epiebnerite) structure are defined by eight-member rings of tetrahedra (see Fig. 7).

The ebnerite structure belongs to the family of "stuffed derivatives" of tridymite (Buerger, 1954). Members of this family exhibit polymorphic variations in configuration and stacking of the tridymite-type layers of tetrahedra. There are many synthetic compounds in this family and some minerals. Pharmazincite, $KZnAsO_4$ (Pekov *et al*., 2017), belongs to this family and is isostructural with megakalsilite, $KAlSiO_4$ (Khomyakov *et al*., 2002). Ebnerite has a cell similar to that of nepheline, $(Na,K)AlSiO_4$, but it differs in polyhedral configuration. The only other mineral with an ABW-type zeolite structure is loomisite, $Ba[Be_2P_2O_8]\cdot H_2O$ (Yang *et al*., 2023b).

Le and Navrotsky (2008) commented on the small difference between the enthalpy of formation of these phases, noting that HEX phases of NH_4MPO_4 (M = Co, Zn) are 3 kJ mol^{-1} more enthalpically stable than ABW phases. This may, in part, explain why epiebnerite has only been found as epitaxial overgrowths on ebnerite.

Acknowledgements

Structures Editor Peter Leverett and two anonymous reviewers are thanked for constructive comments, which improved the manuscript. Ed Davis, current contractor of the

https://doi.org/10.1180/mgm.2024.15 Published online by Cambridge University Press

Rowley mine, is thanked for allowing underground access for the study of the occurrence and the collecting of specimens. This study was funded, in part, by the John Jago Trelawney Endowment to the Mineral Sciences Department of the Natural History Museum of Los Angeles County.

References

Bu, X., Feng, P., Gier, T.E. and Stucky, G.D. (1997) Structural and chemical studies of zeolite ABW type phases: Syntheses and characterizations of an ammonium zincophosphate and an ammonium beryllophosphate zeolite ABW structure. *Zeolites*, **19**, 200–208.

Buerger, M.J. (1954) The stuffed derivatives of the silica structures. *American Mineralogist*, **39**, 600–614.

Donnay, J.H. and Harker, D. (1937) A new law of crystal morphology extending the law of Bravais. *American Mineralogist*, **22**, 446–467.

Frost, R.L., Palmer, S.J. and Pogson, R.E. (2011) Raman spectroscopy of newberyite Mg $(PO_3OH)\cdot 3H_2O$: A cave mineral. *Spectrochimica Acta Part A: Molecular and Biomolecular Spectroscopy*, **79**, 1149–1153.

Gagné, O.C. and Hawthorne, F.C (2015) Comprehensive derivation of bond-valence parameters for ion pairs involving oxygen. *Acta Crystallographica*, **B71**, 562–578.

García-Rodríguez, L., Rute-Pérez, Á., Piñero, J.R. and González-Silgo, C. (2000) Bond-valence parameters for ammonium-anion interactions. *Acta Crystallographica*, **B56**, 565–569.

Harrison, W.T., Sobolev, A.N. and Phillips, M.L. (2001) Hexagonal ammonium zinc phosphate, $(NH_4)ZnPO_4$, at 10 K. *Acta Crystallographica*, **C57**, 508–509.

https://doi.org/10.1180/mgm.2024.15 Published online by Cambridge University Press

Kahlenberg V., Fischer R.X. and Baur W.H. (2001) Symmetry and structural relationships among ABW-type materials. *Zeitschrift für Kristallographie*, **216**, 489–494.

Kampf, A.R., Cooper, M.A., Nash, B.P., Cerling, T., Marty, J., Hummer, D.R., Celestian, A.J., Rose, T.P. and Trebisky, T.J. (2017) Rowleyite, $[Na(NH_4,K)_9Cl_4][V^{5+,4+}{}_2(P,As)O_8]_6 \cdot n[H_2O,Na,NH_4,K,Cl]$, a new mineral with a mesoporous framework structure. *American Mineralogist*, **102**, 1037–1044.

Kampf, A.R., Cooper, M.A., Rossman, R.R., Nash, B.P., Hawthorne, F.C. and Marty, J. (2019a) Davidbrownite-(NH_4), $(NH_4,K)_5(V^{4+}O)_2(C_2O_4)[PO_{2.75}(OH)_{1.25}]_4 \cdot 3H_2O$, a new phosphate-oxalate mineral from the Rowley mine, Arizona, USA. *Mineralogical Magazine*, **84**, 869-877.

Kampf, A.R., Celestian, A.J., Nash, B.P. and Marty, J. (2019b) Phoxite, $(NH_4)_2Mg_2(C_2O_4)(PO_3OH)_2(H_2O)_4$, the first phosphate-oxalate mineral. *American Mineralogist*, **103**, 973–979.

Kampf, A.R., Celestian, A.J., Nash, B.P. and Marty, J. (2021a) Allantoin and natrosulfatourea, two new bat–guano minerals from the Rowley mine, Maricopa County, Arizona, U.S.A. *The Canadian Mineralogist*, **59**, 603-616.

Kampf, A.R., Cooper, M.A., Celestian, A.J., Nash, B.P. and Marty, J. (2021b) Thebaite-(NH_4), $(NH_4,K)_3Al(C_2O_4)(PO_3OH)_2(H_2O)$, a new phosphate-oxalate mineral from the Rowley mine, Arizona, USA. *Mineralogical Magazine* **85**, 379-386.

Kampf, A.R., Cooper, M.A., Celestian, A.J., Ma, C. and Marty, J. (2022a) Dendoraite-(NH_4), a new phosphate-oxalate mineral related to thebaite-(NH_4) from the Rowley mine, Arizona, USA. *Mineralogical Magazine*, **86**, 531-538.

Kampf, A.R., Cooper, M.A., Celestian, A.J., Ma, C. and Marty, J. (2022b) Relianceite-(K), a new phosphate-oxalate mineral related to davidbrownite-(NH_4) from the Rowley mine, Arizona, USA. *Mineralogical Magazine*, **86**, 539–547.

https://doi.org/10.1180/mgm.2024.15 Published online by Cambridge University Press

Kampf, A.R., Ma, C., Hawthorne, F.C. and Marty, J. (2024a) Carboferriphoxite, IMA 2023-097. CNMNC Newsletter 77, *Mineralogical Magazine*, **88**, https://doi.org/.....

Kampf, A.R., Ma, C., Hawthorne, F.C. and Marty, J. (2024b) Ferriphoxite, IMA 2023-096. CNMNC Newsletter 77, *Mineralogical Magazine*, **88**, https://doi.org/.....

Khomyakov, A.P., Nechelyustov, G.N., Sokolova, E., Bonaccorsi, E., Merlino, S. and Pasero, M. (2002) Megakalsilite, a new polymorph of $KAlSiO_4$ from the Khibina alkaline massif, Kola peninsula, Russia: Mineral description and crystal structure. *The Canadian Mineralogist*, **40**, 961–970.

Le, S.N. and Navrotsky, A. (2008) Energetics of formation of alkali and ammonium cobalt and zinc phosphate frameworks. *Journal of Solid State Chemistry*, **181**, 20–29.

Mandarino, J.A. (2007) The Gladstone–Dale compatibility of minerals and its use in selecting mineral species for further study. *The Canadian Mineralogist*, **45**, 1307–1324.

Pekov, I.V., Yapaskurt, V.O., Belakovskiy, D.I., Vigasina, M.F., Zubkova, N.V., Sidorov, E.G. and Della Ventura, G. (2017) New arsenate minerals from the Arsenatnaya fumarole, Tolbachik volcano, Kamchatka, Russia. VII. Pharmazincite, KZnAsO4. *Mineralogical Magazine*, **81**, 1001–1008.

Sergeeva, A.V., Zhitova, E.S and Bocharov, V.N. (2019) Infrared and Raman spectroscopy of tschermigite, $(NH_4)Al(SO_4)_2 \cdot 12H_2O$. *Vibrational Spectroscopy*, **105**, 102983.

Sheldrick, G.M. and IUCr. (2015a) SHELXT – Integrated space-group and crystal-structure determination. *Acta Crystallographica*, **A71**, 3–8.

Sheldrick, G.M. (2015b) Crystal structure refinement with SHELX. *Acta Crystallographica*, **C71**, 3–8.

Števko, M., Sejkora, J., Uher, P., Cámara, F., Škoda, R. and Vaculovič, T. (2018) Fluorarrojadite-(BaNa), $BaNa_4CaFe_{13}Al(PO_4)_{11}(PO_3OH)F_2$, a new member of the

https://doi.org/10.1180/mgm.2024.15 Published online by Cambridge University Press

arrojadite group from Gemerská Poloma, Slovakia. *Mineralogical Magazine*, **82**, 863–876.

Wilson, W.E. (2020) The Rowley mine, Painted Rock Mountains, Maricopa County, Arizona. *Mineralogical Record*, **51**, 181–226.

Yakovenchuk, V.N., Pakhomovsky, Y.A., Konopleva, N.G., Panikorovskii, T.L.. Bazai, A., Mikhailova, J.A., Bocharov, V.N., Ivanyuk, G.Yu. and Krivovichev, S.V. (2018) Batagayite, $CaZn_2(Zn,Cu)_6(PO_4)_4(PO_3OH)_3 \cdot 12H_2O$, a new phosphate mineral from Këster tin deposit (Yakutia, Russia): occurrence and crystal structure. *Mineralogy and Petrology*, **112**, 591–601.

Yang, H., Gu, X., Kampf, A.R., Marty, J., Gibbs. R.B. and Downs. R.T. (2023a) Edwindavisite, IMA 2023-056. CNMNC Newsletter 75, Mineralogical Magazine, **87**, https://doi.org/10.1180/mgm.2023.76

Yang, H., Gu, X., Gibbs, R.B. and Downs, R.T. (2023b) Loomisite, $Ba[Be_2P_2O_8] \cdot H_2O$, the first natural example with the zeolite ABW-type framework, from Keystone, Pennington County, South Dakota, USA. *Mineralogical Magazine*, **87**, 79–85.

https://doi.org/10.1180/mgm.2024.15 Published online by Cambridge University Press

FIGURE CAPTIONS

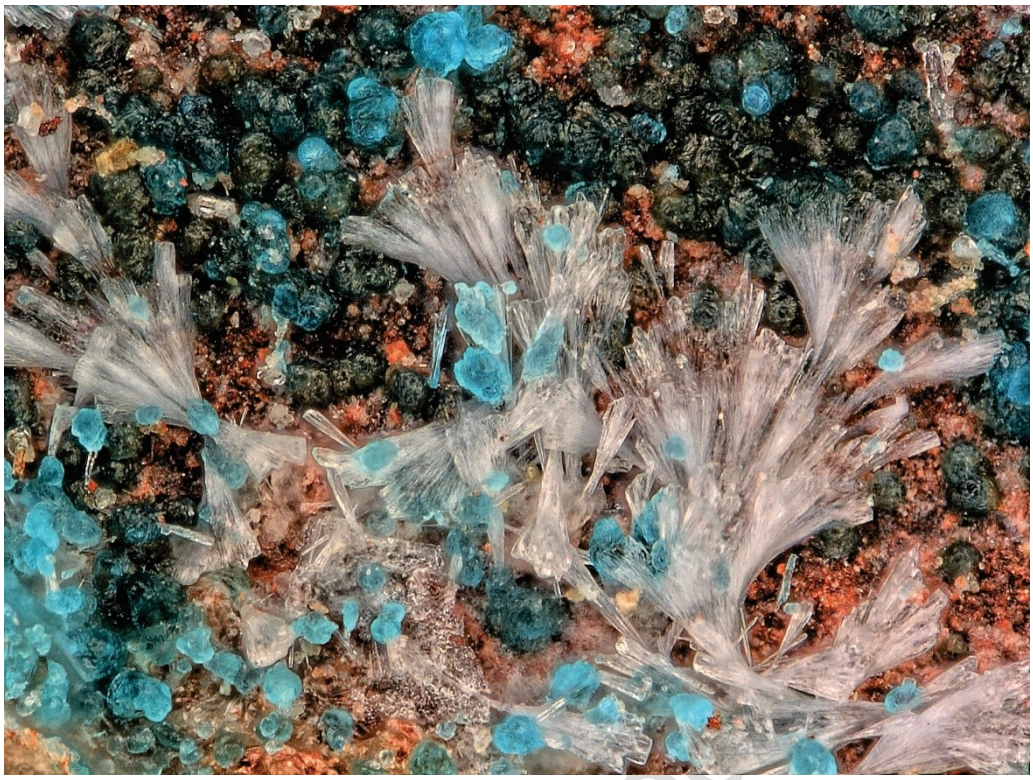

Figure 1: Sprays of ebnerite crystal with blue balls of sampleite. (Specimen #76275; FOV 1.1 mm across)

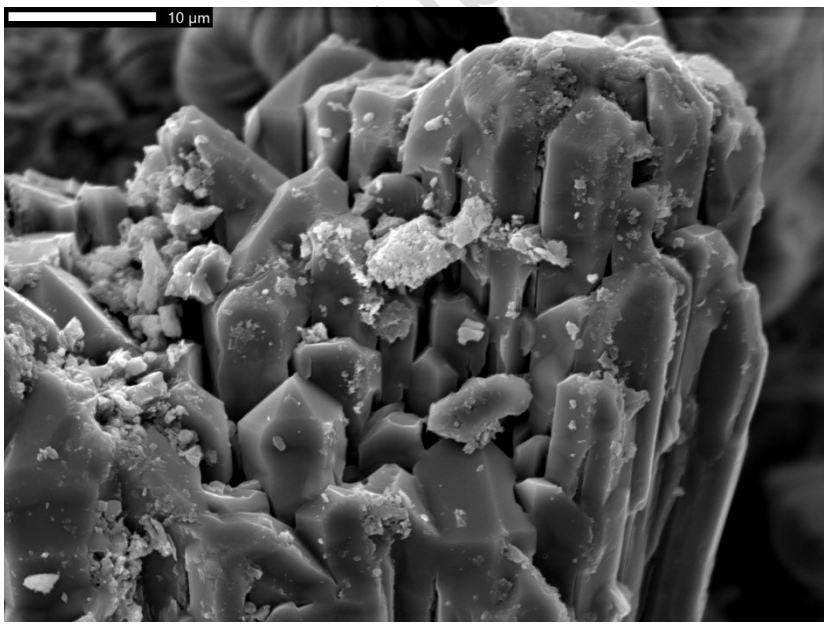

Figure 2. SEM image of the upper portion of a group of ebnerite crystals.

https://doi.org/10.1180/mgm.2024.15 Published online by Cambridge University Press

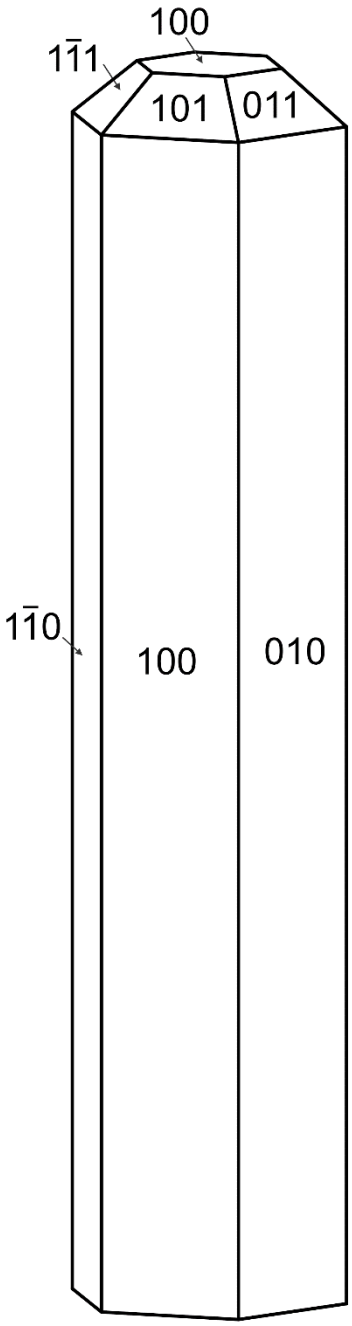

Figure 3. Crystal drawing of ebnerite; clinographic projection in standard orientation.

https://doi.org/10.1180/mgm.2024.15 Published online by Cambridge University Press

Figure 4. Epiebnerite prisms in parallel growth forming serrated ribs growing epitaxially on ebnerite needles. The blue balls are sampleite and the green-yellow crystal with growth hillocks in the background is wulfenite. (Specimen #76294; FOV 0.5 mm across)

https://doi.org/10.1180/mgm.2024.15 Published online by Cambridge University Press

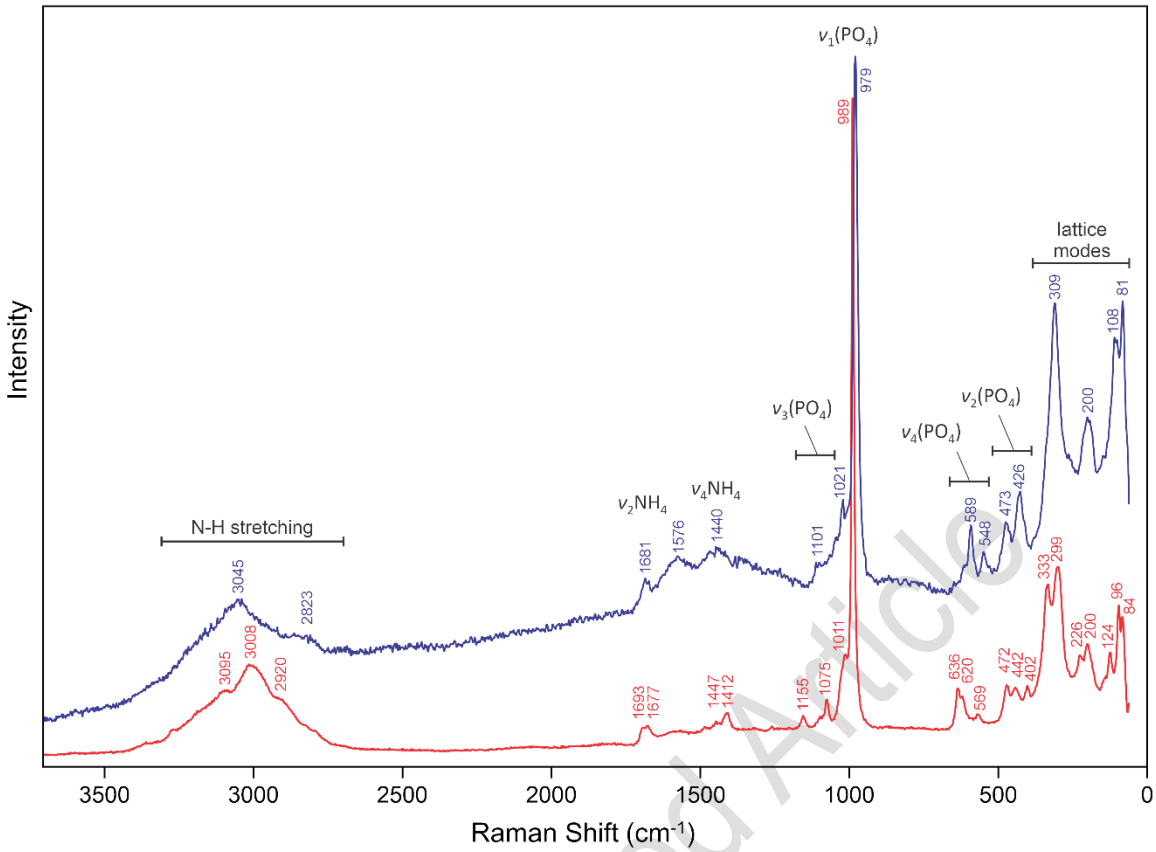

Figure 5. Raman spectra of ebnerite and epiebnerite.

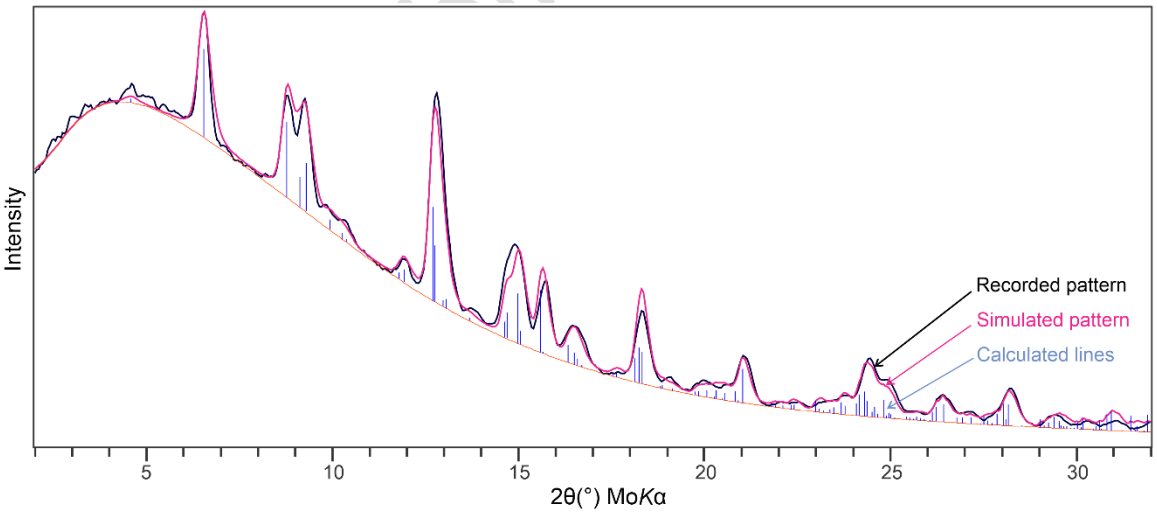

Figure 6. Recorded PXRD of epiebnerite compared with the calculated lines and simulated pattern based on the structure of synthetic ABW-type NH_4ZnPO_4 (Bu *et al.*, 1997).

https://doi.org/10.1180/mgm.2024.15 Published online by Cambridge University Press

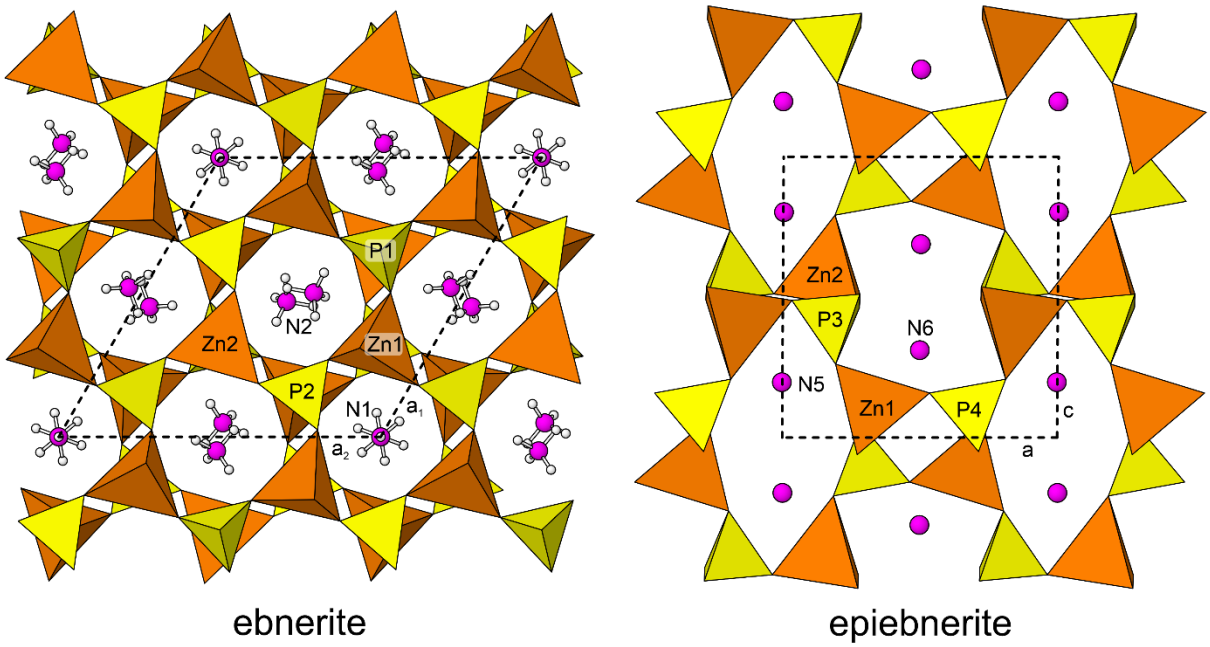

Figure 7. The ebnerite and epiebnerite structures viewed down their channel directions, [001] for ebnerite and [010] for epiebnerite. The unit cell outlines are shown with dashed lines.

https://doi.org/10.1180/mgm.2024.15 Published online by Cambridge University Press

Table 1. Analytical data (wt%) for ebnerite.

Constituent	Mean	Range	S.D.	Probe Standard
$(NH_4)_2O$	12.79	12.72–12.92	0.09	BN
K_2O	1.66	1.37–2.11	0.35	$KAlSi_3O_8$
CuO	3.21	2.87–3.56	0.30	Cu_2O
ZnO	43.49	42.02–44.33	1.02	Zn_2SiO_4
SiO_2	0.92	0.55–1.52	0.42	SiO_2
P_2O_5	38.34	37.85–39.17	0.58	$Ca_5(PO_4)_3F$
Total	100.42			

Table 2. Analytical data (wt%) for epiebnerite.

Constituent	Mean	Range	S.D.	Probe Standard	Norm.
$(NH_4)_2O$	8.29	8.11–8.64	0.24	GaN	9.42
K_2O	6.39	6.18–6.60	0.20	microcline	7.25
ZnO	38.49	38.20–38.82	0.29	ZnO	43.72
CuO	0.92	0.90–0.94	0.02	Cu metal	1.05
P_2O_5	33.96	33.45–34.52	0.56	apatite	38.57
Total	88.05				100.01

https://doi.org/10.1180/mgm.2024.15 Published online by Cambridge University Press

Table 3. Data collection and structure refinement details for ebnerite.

Diffractometer	Rigaku Xtalab Synerg D/S
X-ray radiation	Cu$K\alpha$ (λ = 1.54184)
Temperature	293(2) K
Formula derived from SREF	$[(NH_4)_{0.94}K_{0.05})]_{\Sigma 0.99}Zn_{0.94}(P_{0.95}O_4)$
Space group	$P6_3$ (#173)
Unit cell dimensions	a = 10.67051(16) Å
	c = 8.7140(2) Å
V	859.25(3) Å^3
Z	8
Density (for above formula)	2.679 g cm^{-3}
Absorption coefficient	10.745 mm^{-1}
F(000)	688.6
Crystal size	40 × 30 × 20 µm
θ range	4.79 to 77.66°
Index ranges	$-13 \le h \le 8$, $-13 \le k \le 13$, $-10 \le l \le 11$
Refls collected / unique	9691 / 1207; R_{int} = 0.056
Reflections with $I > 2\sigma I$	1168
Completeness to θ = 77.66°	99.8%
Refinement method	Full-matrix least-squares on F^2
Parameters / restraints	107 / 15
GoF	1.040
Final R indices [$I > 2\sigma I$]	R_1 = 0.0372, wR_2 = 0.0940
R indices (all data)	R_1 = 0.0382, wR_2 = 0.0952
Absolute structure parameter	0.06(8)
Largest diff. peak / hole	+0.45 / –0.87 e/A^3

$R_{int} = \Sigma|F_o^2\text{-}F_o^2(\text{mean})|/\Sigma[F_o^2]$. GoF = $S = \{\Sigma[w(F_o^2 - F_c^2)^2]/(n-p)\}^{1/2}$. $R_1 = \Sigma||F_o|\text{-}|F_c||/\Sigma|F_o|$. $wR_2 = \{\Sigma[w(F_o^2 - F_c^2)^2]/\Sigma[w(F_o^2)^2]\}^{1/2}$; $w = 1/[\sigma^2(F_o^2) + (aP)^2 + bP]$ where a is 0.0789, b is 0 and P is $[2F_c^2 + \text{Max}(F_o^2,0)]/3$.

https://doi.org/10.1180/mgm.2024.15 Published online by Cambridge University Press

Table 4. Atom positions, site occupancies and displacement parameters (Å)^2 for ebnerite.

	Site occupancy	*x*/*a*	*y*/*b*	*z*/*c*	U_{eq}
N1	$N_{0.81(2)}K_{0.19(2)}$	0	0	0.6679(7)	0.018(2)
H1a	$H_{0.81(2)}$	0	0	0.770(5)	0.022
H1b	$H_{0.81(2)}$	-0.030(9)	-0.086(6)	0.629(7)	0.022
N2	$N_{0.990(13)}K_{0.010(13)}$	0.4654(5)	-0.0500(5)	0.1598(8)	0.020(2)
H2a	$H_{0.990(13)}$	0.424(7)	-0.078(7)	0.067(5)	0.024
H2b	$H_{0.990(13)}$	0.419(6)	-0.012(6)	0.213(7)	0.024
H2c	$H_{0.990(13)}$	0.556(4)	0.024(5)	0.143(9)	0.024
H2d	$H_{0.990(13)}$	0.470(7)	-0.118(5)	0.209(7)	0.024
Zn1	$Zn_{0.945(10)}$	0.14857(8)	0.32567(7)	0.46454(11)	0.0124(3)
Zn2	$Zn_{0.941(12)}$	1/3	2/3	0.83709(16)	0.0124(5)
P1	$P_{0.95(2)}$	1/3	2/3	0.4496(3)	0.0125(10)
P2	$P_{0.956(15)}$	0.32647(13)	0.17949(14)	0.3436(2)	0.0110(8)
O1	$O_{1.00}$	1/3	2/3	0.6190(12)	0.047(3)
O2	$O_{1.00}$	0.2886(5)	0.5160(4)	0.3872(6)	0.0229(12)
O3	$O_{1.00}$	0.3178(4)	0.2243(5)	0.1794(5)	0.0213(11)
O4	$O_{1.00}$	0.4753(5)	0.2846(5)	0.4116(6)	0.0231(11)
O5	$O_{1.00}$	0.2091(4)	0.1833(4)	0.4418(5)	0.0190(11)
O6	$O_{1.00}$	0.3012(5)	0.0246(5)	0.3456(6)	0.0234(11)

	U^{11}	U^{22}	U^{33}	U^{23}	U^{13}	U^{12}
N1	0.019(2)	0.019(2)	0.016(4)	0	0	0.0095(12)
N2	0.020(3)	0.024(3)	0.015(3)	0.001(3)	0.000(2)	0.011(2)
Zn1	0.0133(4)	0.0125(4)	0.0117(6)	0.0002(4)	0.0003(4)	0.0065(3)
Zn2	0.0126(6)	0.0126(6)	0.0120(9)	0	0	0.0063(3)
P1	0.0137(11)	0.0137(11)	0.0100(17)	0	0	0.0069(6)
P2	0.0116(10)	0.0105(10)	0.0105(11)	0.0003(6)	0.0020(6)	0.0053(6)
O1	0.067(5)	0.067(5)	0.007(6)	0	0	0.034(2)
O2	0.022(2)	0.014(2)	0.032(3)	0.0016(16)	0.0078(18)	0.0081(17)
O3	0.030(2)	0.0214(19)	0.011(2)	-0.0007(17)	-0.0006(16)	0.0115(17)
O4	0.017(2)	0.029(2)	0.019(2)	-0.0072(18)	-0.0017(17)	0.0084(19)
O5	0.0197(19)	0.0219(19)	0.019(3)	0.0029(18)	0.0065(18)	0.0131(15)
O6	0.032(2)	0.018(2)	0.022(2)	0.0040(18)	0.010(2)	0.0139(17)

https://doi.org/10.1180/mgm.2024.15 Published online by Cambridge University Press

Table 5. Selected bond lengths (Å) and angles (°) for ebnerite.

N1–O5 (×3)	2.885(6)	Zn1–O5	1.935(4)
N1–O3 (×3)	3.021(4)	Zn1–O2	1.943(5)
N1–O5 (×3)	3.183(7)	Zn1–O6	1.949(5)
N1–O6 (×3)	3.457(6)	Zn1–O3	1.951(5)
<N1–O>	3.011	<Zn1–O>	1.945
N2–O6	2.778(7)	Zn2–O1	1.900(10)
N2–O4	2.785(7)	Zn2–O4 (×3)	1.949(5)
N2–O2	2.816(7)	<Zn2–O>	1.937
N2–O3	2.876(6)		
N2–O2	3.223(7)	P1–O1	1.476(10)
N2–O4	3.417(8)	P1–O2 (×3)	1.530(4)
N2–O1	3.562(5)	<P1–O>	1.517
N2–O4	3.596(8)		
N2–O6	3.619(8)	P2–O3	1.526(5)
N2–O2	3.619(7)	P2–O4	1.533(5)
N2–O5	3.676(7)	P2–O5	1.534(4)
<N2–O>	3.132	P2–O6	1.536(4)
		<P2–O>	1.532

Hydrogen bonds

D–H···*A*	*D*–H	H···*A*	*D*···*A*	<DHA
N1-H1a···O5 (×3)	0.89(4)	2.58(2)	3.183(6)	125.4(7)
N1-H1b···O5	0.87(4)	2.11(4)	2.885(6)	147(7)
N2-H2a···O4	0.89(3)	1.93(4)	2.785(7)	160(7)
N2-H2b···O6	0.90(3)	1.89(3)	2.778(7)	167(5)
N2-H2c···O3	0.90(3)	2.10(4)	2.876(6)	143(5)
N2-H2d···O2	0.86(3)	1.99(4)	2.816(7)	159(6)

Table 6. Bond valences analysis for ebnerite. Values are in valence units (*vu*).

	N1$^{\times 3\downarrow}$	N2	Zn1	Zn2	P1	P2	Σ
O1		0.03$^{\times 3\rightarrow}$		0.57	1.45		2.11
O2		0.20, 0.07, 0.02	0.51		1.27$^{\times 3\downarrow}$		2.07
O3	0.12	0.17	0.50			1.28	2.07
O4		0.22, 0.04, 0.02		0.50$^{\times 3\downarrow}$		1.26	2.04
O5	0.17, 0.08		0.52			1.25	2.02
O6	0.04	0.22, 0.02	0.50			1.25	2.03
Σ	1.23	1.03	2.03	2.07	5.25	5.03	

Bond-valence parameters for NH_4^+–O are from Garcia-Rodriguez *et al*. (2000); all others are from Gagné and Hawthorne (2015). The cation sites were modelled using full occupancies by their dominant cations.

https://doi.org/10.1180/mgm.2024.15 Published online by Cambridge University Press